The miR-17-92 cluster expands multipotent hematopoietic progenitors whereas imbalanced expression of its individual oncogenic miRNAs promotes leukemia in mice

Yanmei Li,[1,2] Laura M. Vecchiarelli-Federico,[1,2] You-Jun Li,[1,2] Sean E. Egan,[3,4] David Spaner,[1,2] Margaret R. Hough,[2,5] and Yaacov Ben-David[1,2]

[1]Department of Medical Biophysics, University of Toronto, Toronto, ON; [2]Molecular and Cellular Biology, Sunnybrook Health Sciences Centre, Toronto, ON; [3]Department of Medical Genetics, University of Toronto, Toronto, ON; [4]Program in Developmental and Stem Cell Biology, Hospital for Sick Children, Toronto, ON; and [5]Institute of Medical Science, University of Toronto, Toronto, ON

The miR-17-92 cluster and its 6 encoded miRNAs are frequently amplified and aberrantly expressed in various malignancies. This study demonstrates that retroviral-mediated miR-17-92 overexpression promotes expansion of multipotent hematopoietic progenitors in mice. Cell lines derived from these miR-17-92–overexpressing mice are capable of myeloid and lymphoid lineage differentiation, and recapitulate the normal lymphoid phenotype when transplanted to nonobese diabetic/severe combined immunodeficiency mice. However, overexpression of individual miRNAs from this locus, miR-19a or miR-92a, results in B-cell hyperplasia and erythroleukemia, respectively. Coexpression of another member of this cluster miR-17, with miR-92a, abrogates miR-92a–induced erythroleukemogenesis. Accordingly, we identified several novel miR-92a and miR-17 target genes regulating erythroid survival and proliferation, including *p53*. Expression of this critical target results in marked growth inhibition of miR-92a erythroleukemic cells. In both murine and human leukemias, p53 inactivation contributed to the selective overexpression of oncogenic miR-92a and miR-19a, and down-regulation of tumor-suppressive miR-17. This miR-17-92 expression signature was also detected in p53$^-$ B-cell chronic lymphocytic leukemia patients displaying an aggressive clinical phenotype. These results revealed that imbalanced miR-17-92 expression, also mediated by p53, directly transforms the hematopoietic compartment. Thus examination of such miRNA expression signatures should aid in the diagnosis and treatment of cancers displaying *miR-17-92* gene amplification. (*Blood*. 2012;119(19):4486-4498)

Introduction

Hematopoiesis is regulated by genes governing cellular proliferation, differentiation, and apoptosis. Recent studies demonstrated that microRNAs (miRNAs), an important class of small non-protein–coding RNA molecules, play a critical role during hematopoiesis by post-transcriptionally regulating the expression of critical genes involved in these processes.[1,2] Many miRNAs are specifically expressed in hematopoietic cells and their expression is dynamically regulated during hematopoiesis and lineage commitment.[1,3] Therefore it is not surprising that aberrant miRNA expression has frequently been observed in a wide variety of human cancers[4-6] and has been implicated in the initiation and progression of both solid and hematopoietic tumors.[7,8] Although the oncogenic and tumor-suppressor functions of miRNAs are not completely understood, it is known that miRNAs regulate the expression of key genes governing malignant transformation.[9,10]

Recent studies revealed that aberrant miRNA expression may directly contribute to tumorigenesis. Our group identified the *miR-17-92* locus as a retroviral insertion site in a subset of erythroleukemias induced in *p53* knockout mice.[11] The miR-17-92 cluster produces a single polycistronic primary transcript processed to yield 6 individual mature miRNAs; miR-17, miR-18, miR-19a, miR-19b, miR-20, and miR-92a. This cluster is located on human chromosome 13q31, a genomic region frequently amplified in human lymphomas and solid tumors, including tumors of the breast, colon, lung, pancreas, prostate, and stomach.[5,8,12,13] Evidence for the importance of miR-17-92 overexpression in tumor initiation and progression is strengthened by the observation that transgenic expression of this cluster in lymphocytes leads to a lymphoproliferative disorder in mice.[4] Although miR-17-92 can function as an oncogene in lymphoma[5] and lung cancer,[14] miR-17-92 members can also suppress tumor formation in the breast and ovary,[15] which suggests functional distinctions among the individual members. Moreover, despite an increasing number of in vitro studies suggesting an oncogenic role for miRNAs similar to miR-17-92, very few animal models exist to directly test this theory in vivo. To explore the role of each of the 6 constituent members of miR-17-92 in malignant transformation, we infected newborn mice with retroviruses to directly overexpress the entire miR-17-92 cluster or its individual miRNAs. Here we demonstrate for the first time, that although balanced expression of all 6 members of this cluster expands multipotent hematopoietic progenitors, alteration in the balanced expression of individual miR-17-92 members is required to promote leukemogenesis.

Submitted September 8, 2011; accepted March 11, 2012. Prepublished online as *Blood* First Edition paper, March 26, 2012; DOI 10.1182/blood-2011-09-378687.

The online version of this article contains a data supplement.

The publication costs of this article were defrayed in part by page charge payment. Therefore, and solely to indicate this fact, this article is hereby marked "advertisement" in accordance with 18 USC section 1734.

Methods

Molecular construction of retroviral expression vectors

MiR-17-92 and its individual members; miR-17-5p, miR-19a, and miR-92a were amplified using real-time polymerase chain reaction (PCR) and cloned between the *BglII* and *HpaI* restriction sites of the pMSCV-Hyg-IRES-GFP retroviral expression vector, a kind gift from Dr Dan Dumont, University of Toronto (supplemental Figure 1, available on the *Blood* Web site; see the Supplemental Materials link at the top of the online article). Primer sequences are listed in supplemental Figure 11.

Mice

Animal studies/procedures were approved by the Sunnybrook Health Sciences Center animal care committee. Retroviruses were injected intraperitoneally into newborn Balb/c mice and monitored daily. The transplantation study was performed using CB17–nonobese diabetic (NOD)/severe combined immunodeficiency (SCID) mice.

Establishment of miR-17-92 cell lines

Hematopoietic progenitor cell lines (CSC1 and CSC2) were derived from the spleens of miR-17-92–overexpressing mice. Briefly, splenocytes from these mice were seeded at 1×10^6 cells/mL in α-minimum essential media (α-MEM; Sigma-Aldrich) supplemented with 20% fetal bovine serum (FBS; Gibco), 100 U/mL penicillin/streptomycin (Gibco), 10^{-4} mol/L 2-mercaptoethanol (Sigma-Aldrich), 100 ng/mL of SCT (R&D Systems), 100 ng/mL IL-3, and 1 U/mL of erythropoietin (Epo; Boehringer Mannheim). After 2 months in culture, nonadherent small-round cells became stromal-cell independent and grew as cell lines in culture without IL-3 and Epo. The same strategy was used to derive erythroleukemic cell lines SB1-SB5 from miR-92a–overexpressing spleens.

Cell lines

Human leukemic cell lines K562, HEL, HL-60, and TK6 were grown in RPMI 1640 (Gibco) containing 10% FBS (Gibco) at 37°C in 5% CO_2. NIH-3T3 cells were grown in α-MEM (Gibco) containing 10% FBS (Gibco).

B-CLL cell isolation, cytogenetics and irradiation

Heparinized blood was obtained from healthy volunteers and consenting chronic lymphocytic leukemia (CLL) patients diagnosed by persistent monoclonal expansion of $CD19^+/CD5^+/IgM^{lo}$ lymphocytes, not receiving treatment for > 3 months at the time of isolation and analysis. Protocols were approved by the Sunnybrook Ethics Review Board and informed consent was obtained in compliance with the Declaration of Helsinki. Clinical characteristics of B-CLL patients are described in supplemental Table 3. Normal B cells and B-CLL cells were isolated by negative selection with the Rosette Sep Human B-cell enrichment cocktail (StemCell Technologies) and density centrifugation with Ficoll-Paque (Amersham Pharmacia Biotech). This method of purification yields percentages of $CD19^+$ and $CD19^+/CD5^+$ cells, $> 98\%$ and 96%, respectively. Irradiation experiments were performed in PBS (Sigma-Aldrich) for 13.5 seconds at 1.6 $Gymin^{-1}$ (total dose of 5 Gy). Cells were exposed to ionizing radiation for 10 minutes, 16 Gy, or 15 minutes, 24 Gy. After irradiation, proteins were isolated for the detection of p53 and p21, as previously described.[11]

In vitro colony formation assay

The frequency of CFU-GM, CFU-GEMM, and BFU-E in spleens was analyzed using methylcellulose-based colony assays performed using methylcellulose (MethoCultM-3434; StemCell Technologies) presupplemented with 100 ng/mL murine IL-3, 200 ng/mL murine kit ligand (KL), 2 U/mL human EPO, and 0.2mM hemin3′. Splenocytes were isolated, and pooled within each test group. Cells (1×10^5) were plated in triplicate wells in 35-mm dishes (Costar). Plates were incubated at 37°C in a humidified atmosphere containing 6.5% CO_2. Absolute numbers of colony-forming units (CFUs), containing more than 50 cells, were calculated after 5 to 14 days of culture by multiplying the number of CFUs per 1×10^5 cells by the total cellularity of spleen.

Transfection and transduction

See supplemental Methods.

Quantitative real-time PCR and Western blot analysis

Precursor miRNA (pri-miRNA) and the mRNA levels of *p53*, *gata-1*, *bcl-2*, *STAT-5*, *jak2*, *miR-17*, *miR-18a*, *miR-19a*, *miR-20*, *miR-19b*, and *miR-92a* were determined using real-time PCR analysis with SYBR (Applied Biosystems). β-actin was used as a normalization control in all RT-PCR experiments. Total RNA was extracted using Trizol (Sigma-Aldrich) and treated with DNaseI (Sigma-Aldrich). CDNA was generated using SuperScript II First-Strand Synthesis System (Invitrogen). PCR analyses were performed using the SYBR Green JumpStart Taq ReadyMix (Sigma-Aldrich) according to the manufacturer's protocol using the ABI PRISM 7000 machine (Applied Biosystems). See supplemental Figure 11 for primer sequences. Proteins were isolated as previously described (Cui et al[11]). Gata-1, p53, Bcl-2, STAT-5, Jak2, p53, and p21 antibodies (Santa Cruz Biotechnology Inc) were used at 1:1000 dilutions.

Survival and statistical analysis

See supplemental Methods.

Histology

Tissues fixed with 10% formalin (Sigma-Aldrich) were stained with H&E or periodic acid-Schiff. Images were obtained using a Leica DM LB2 microscope 10× objective, Leica DFC 300FX camera and Leica Application Suite Version 3.1.0 software (Leica Microsystems).

Hematocrit measurements

See supplemental Methods.

Transplantation experiments

CB17-NOD/SCID mice were injected intravenously with 5×10^6 $ckit^+/Sca1^+$ sorted CSC1 cells in 500 mL of PBS (Sigma-Aldrich). Noninfected and PBS-injected mice were used as controls. Quantitative real-time PCR analysis confirmed the presence of CSC1 donor DNA in CSC1 transplanted NOD/SCID mice. Briefly, serial dilutions of CSC1 DNA, carrying the Y chromosome, were added to NOD/SCID splenic DNA and expression of the Y chromosome specific gene, *SRY*, was quantified, as previously described.

Flow cytometric analysis

Immunofluorescence staining was performed to determine cell surface marker expression on the splenocytes of control and infected mice, as well as their derivative cell lines. Cells (1×10^6) were incubated with blocking antibody (eBiosciences) for 15 minutes at 4°C. Cells were stained with primary antibodies for 30 minutes on ice. Primary antibodies were as follows, phycoerythrin (PE)–conjugated anti–mouse c-kit, CD71, Gr1, Mac1, CD4, or CD19, allophycocyanin (APC)–conjugated anti–mouse TER-119, Sca1, B220, and CD8 (eBiosciences). Cells were washed and resuspended in fluorescence-activated cell sorter (FACS) buffer. Propidium iodide (PI) 1 μg/mL was added to exclude dead cells (Sigma-Aldrich). All flow cytometric analyses were performed on a FACSCalibur (Becton Dickinson). Data were analyzed with the FlowJo Version 9.3.0 software (TreeStar).

Apoptosis analysis

See supplemental Methods.

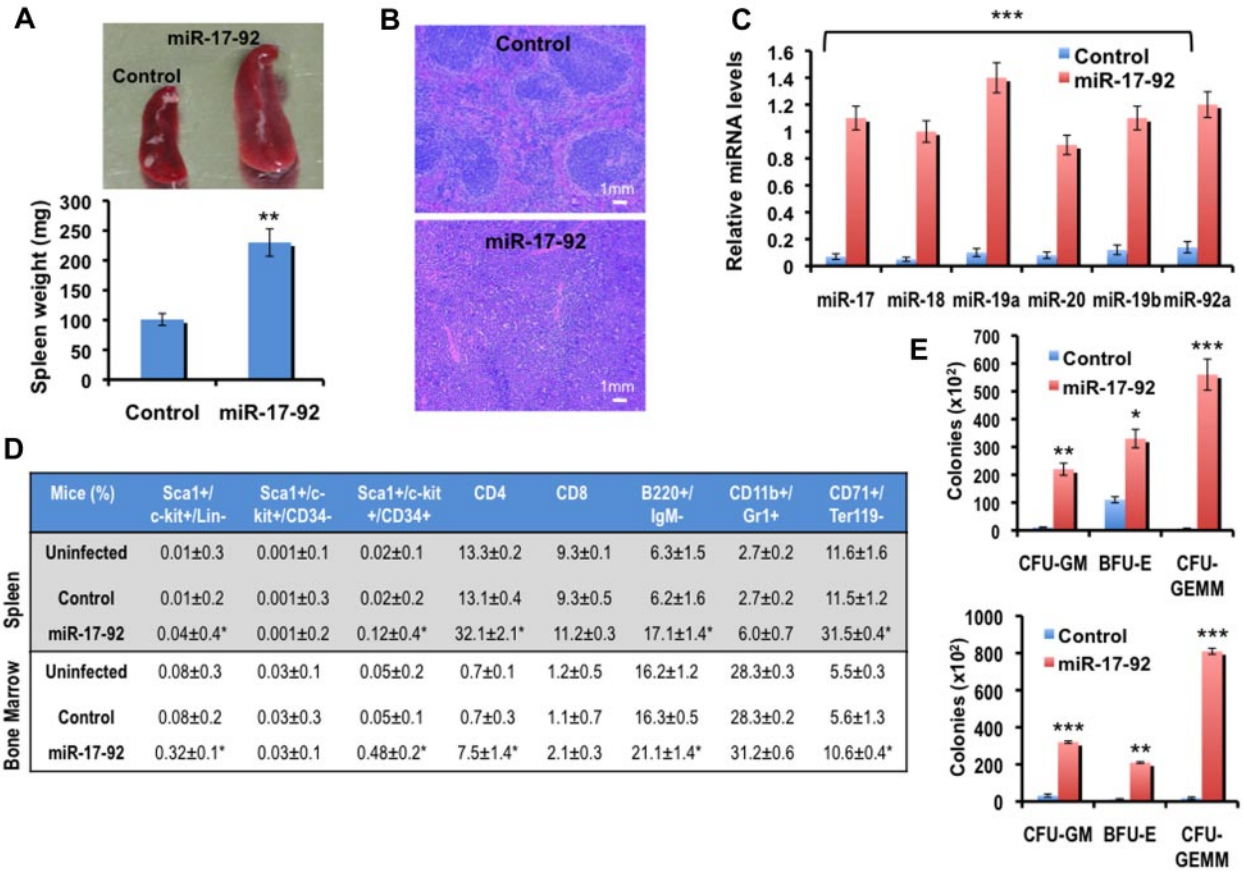

	Mice (%)	Sca1+/c-kit+/Lin-	Sca1+/c-kit+/CD34-	Sca1+/c-kit+/CD34+	CD4	CD8	B220+/IgM-	CD11b+/Gr1+	CD71+/Ter119-
Spleen	Uninfected	0.01±0.3	0.001±0.1	0.02±0.1	13.3±0.2	9.3±0.1	6.3±1.5	2.7±0.2	11.6±1.6
	Control	0.01±0.2	0.001±0.3	0.02±0.2	13.1±0.4	9.3±0.5	6.2±1.6	2.7±0.2	11.5±1.2
	miR-17-92	0.04±0.4*	0.001±0.2	0.12±0.4*	32.1±2.1*	11.2±0.3	17.1±1.4*	6.0±0.7	31.5±0.4*
Bone Marrow	Uninfected	0.08±0.3	0.03±0.1	0.05±0.2	0.7±0.1	1.2±0.5	16.2±1.2	28.3±0.3	5.5±0.3
	Control	0.08±0.2	0.03±0.3	0.05±0.1	0.7±0.3	1.1±0.7	16.3±0.5	28.3±0.2	5.6±1.3
	miR-17-92	0.32±0.1*	0.03±0.1	0.48±0.2*	7.5±1.4*	2.1±0.3	21.1±1.4*	31.2±0.6	10.6±0.4*

Figure 1. Overexpression of miR-17-92 in mice leads to expansion of multipotent hematopoietic progenitor cells. (A) A representative photograph (top panel) and average spleen weights of empty vector control vector (n = 6) and miR-17-92 mice (n = 8), 16 weeks after infection (bottom panel), where error bars represent SD; $^{**}P < .005$. (B) H&E stained paraffin sections of spleens from empty vector control and miR-17-92 mice 16 weeks after infection (scale bar, 1 mm). Data are representative sections from 3 staining experiments. (C) Quantitative RT-PCR analysis of precursor miR-17-92 expression in the spleens isolated from empty vector control (n = 4) and miR-17-92 mice (n = 4) 16 weeks after infection. Results were normalized relative to β-actin expression in all experimental samples. Each experiment was performed in quadruplicate, where error bars represent SD; $^{***}P < .0005$. (D) Frequency of hematopoietic cell surface marker expression, as a percentage of total splenocytes (top panel) and bone marrow cells (bottom panel) isolated from uninfected (n = 3), empty vector control (n = 4), and miR-17-92 mice (n = 4). Values represent the mean % ± SD; $^{*}P < .05$ (E) in vitro colony assays displaying the kinetics of CFU colony expansion of miR-17-92 or empty vector control injected mice (n = 6) splenocytes (top panel) and BM cells (bottom panel). Three CFU types were scored: CFU-GM, BFU-E, and CFU-GEMM. Colony counts were performed in triplicate after 5 to 14 days of culture, where error bars represent SD; $^{*}P < .05$, $^{**}P < .005$, and $^{***}P < .0005$.

Luciferase reporter assay

NIH-3T3 cells overexpressing miR-92a or miR-17 were plated into 12-well plates at 3 to 4×10^5 cells/well 24 hours before transfection. pMIR-REPORT luciferase reporter plasmid 0.2 μg (Ambion) containing potential miRNA binding sequences or mutant variations, and 0.8 μg miR-92a or miR-17 expressing pMSCV vector were cotransfected into each well using Lipofectamine 2000 transfection reagent (Invitrogen) in 4 triplicates. Mutagenesis of these miRNA-binding sites was carried out using the QuickChangeXL mutagenesis kit (Stratagene) following the manufacturer's protocol. Relative luciferase units (RLU) were measured 48 hours after transfection using the Luciferase Reporter Assay System (Ambion) on a Synergy 2 microplate reader (BioTek Instruments).

Results

Retroviral overexpression of miR-17-92 in mice expands multipotent hematopoietic progenitors

To directly test the oncogenic potential of miR-17-92 in vivo, pMSCV-EGFP retroviral vectors encoding the miR-17-92 cluster or empty vector control (supplemental Figure 1A) were injected into newborn Balb/c mice. Sixteen weeks after infection, mice injected with miR-17-92–expressing virus developed a 2-fold increase in spleen size (Figure 1A) and displayed disrupted splenic architecture, specifically, a loss of follicular structure and expansion of red pulp regions (Figure 1B). Despite this splenic abnormality, miR-17-92–infected mice failed to display other characteristics of disease (ie, low hematocrit and weight values) during a 1-year observation period. Quantitative PCR, performed 16 weeks after infection, confirmed a 10- to 20-fold increase in the expression of precursor miR-17-92 in the spleens of miR-17-92–injected mice, compared with empty vector control mice (Figure 1C). Flow cytometric analysis of isolated miR-17-92 overexpressing splenocytes and bone marrow (BM) cells demonstrated a significant increase in the fraction of cells expressing multipotent hematopoietic progenitor cell surface markers, relative to vector alone infected mice (Figure 1D). Although EGFP expression could not be used as a positive selection marker because processing of the miRNA transcript by Drosha probably destabilizes the RNA encoding EGFP.[16]

A colony-forming cell assay was performed to further investigate the effects of miR-17-92 overexpression on this hematopoietic progenitor population. CFUs representing granulocyte, macrophage (CFU-GM); granulocyte, erythrocyte, macrophage, and

megakaryocyte (CFU-GEMM), and burst forming units erythroid (BFU-E) were enumerated after growth in conditioned methylcellulose. The number of spleen and BM-derived CFU-GM, and CFU-GEMM, and BFU-E colonies significantly increased in miR-17-92–overexpressing mice compared with control animals (Figure 1E).

Isolated splenocytes from miR-17-92–overexpressing mice were also grown in suspension cultures supplemented with SCF, IL-3, Epo, and high serum levels. Under these culture conditions, we observed the survival and slow expansion of nonadherent, small, round cells phenotypically distinct from the adherent stromal cells characteristically seen in most cultures of splenic origin. After 1 month in culture, this miR-17-92–overexpressing nonadherent population became stromal cell independent and 2 cell lines were established, CSC1 ($CD34^{hi}$) and CSC2 ($CD34^{lo}$; Figure 2A-B). The predominance of c-kit^+/$Sca1^+$/$CD135^+$ (Flt3), c-kit^+/$Sca1^+$/$CD34^+$, and $CD48^-$/$CD150^-$/$CD135^+$ populations in CSC1 cells suggested the predominance of multipotent hematopoietic progenitor cells.[17] These cells also express CD41, a marker of definitive hematopoiesis and myeloid progenitors,[18] and CD38, a marker of long-term reconstituting hematopoietic cells (Figure 2B).[19] A limiting dilution assay followed by flow cytometric analysis demonstrated that 5% of CSC1 cells were capable of self-renewal and differentiation, generating new cultures almost indistinguishable from the parental line. Similar results were also observed with the CSC2 cell line (data not shown).

To further characterize the multipotent potential of these progenitor cell lines, CSC1 cells were cultured on methylcellulose supplemented with various erythroid/myeloid-inducing growth factors. After 10 to 14 days of culture, significant numbers of colonies consisting of CFU-G, CFU-GEMM, CFU-M, and BFU-E colonies were detected (Figure 2C). Histologic staining with May-Giemsa validated the identification of these colonies (supplemental Figure 2), and confirmed the ability of CSC1 cells to undergo differentiation into various erythroid/myeloid cells in vitro. To assess the in vivo potential of CSC1 cells to differentiate into lymphoid cells, ckit+/Sca1+ sorted CSC1 cells were transplanted into lymphoid-deficient NOD/SCID mice. Spleen weights of CSC1-injected NOD/SCID mice were approximately 2-fold larger, 4 months after injection (Figure 2D), and demonstrated the presence of mature B and T cells relative to control mice (Figure 2E). Moreover, the expected 2:1 ratio of CD4:CD8 cells was observed in CSC1-injected NOD/SCID mice, recapitulating a normal lymphoid phenotype.[20] Because the CSC1 cell line was originally derived from splenocytes of a male mouse, quantitative RT-PCR, detecting the Y chromosome specific gene, *SRY*,[21] confirmed that approximately 20% of the splenocytes were of CSC1 origin (Figure 2F). Combined, these studies demonstrate that miR-17-92 overexpression expands a multipotent hematopoietic progenitor population capable of undergoing differentiation to lymphoid and myeloid cells.

Induction of erythroleukemia in miR-92a–overexpressing mice

The 6 miRNAs produced by the miR-17-92 cluster (supplemental Figure 1B) are associated with malignancy, specifically miR-92a, which has been implicated as an oncogene. To test the direct contribution of this miRNA in tumorigenesis, miR-92a was retrovirally expressed in newborn mice. Quantitative PCR confirmed a 20-fold increase in precursor miR-92a expression 12 weeks after infection, compared with mice infected with the empty vector control (Figure 3A). After injection, 18 control and 26 miR-92a–overexpressing mice were monitored for 25 weeks. During this period, 23 (89%) miR-92a infected mice succumbed to disease, whereas all control mice remained healthy (Figure 3B). MiR-92a mice developed a severe disease associated with massive weight loss, anemia, and spleens 15-fold larger than control mice (Figure 3C), with a distinguished white pulp and expansion of the red pulp region 12 weeks after infection (Figure 3D). Flow cytometric analysis revealed spleens of miR-92a–infected mice displayed a significant increase in the number of c-kit^+/$CD71^+$/$Ter119^-$ cells (Figure 3E), suggesting the occurrence of erythroleukemia. We also detected a significant increase in the number of $CD11b^+$ myeloid cells, compared with empty vector control mice (Figure 3E). To investigate the effects of miR-92a overexpression in hematopoietic progenitor differentiation, a colony-forming cell assay was performed to quantify changes in the number of CFU-GM, CFU-GEMM, and BFU-Es. The number of spleen-derived BFU-Es increased 8-fold in miR-92a–infected mice compared with empty vector control mice, whereas the frequencies of CFU-GM and CFU-GEMMs remained unchanged (Figure 3F). Isolated splenocytes from leukemic miR-92a–overexpressing mice were cultured in the presence of Epo, SCF, and IL3. Under these culture conditions, miR-92a–induced tumors (LSB1-LSB5) gave rise to 5 cell lines (termed SB1-SB5), respectively. Southern blot analysis, using the green fluorescence protein (GFP) sequence as a probe, present in the miR-92a retrovirus, demonstrated the oligoclonal origin of these cell lines (data not shown). Flow cytometric analysis of SB1-SB5 cell lines revealed expression of c-kit, CD71, and Ter119 (supplemental Table 1), further confirming the incidence of erythroleukemia in mice overexpressing miR-92a. The oncogenic role of miR-92a was further supported by transfer of SB1 cells into NOD/SCID mice. After SB1 cell injection, mice display signs of disease at 3 weeks, and die approximately 5 weeks after injection. These mice develop splenomegaly, anemia, and express characteristic cell surface markers of erythroleukemia, compared with the appropriate controls (supplemental Figure 3).

Overexpression of miR-19a in mice causes B cell expansion

Recent studies have demonstrated that cooperation between miR-17-92 and c-Myc is critical for lymphoma induction in a mouse model of B-cell lymphoma.[22] miR-19 is the critical lymphoma-inducing member of this cluster that cooperates with c-Myc to inhibit apoptosis through down-regulation of phosphatase and tensin homolog (PTEN).[22,23] Notably, the sequences of miR-19a and miR-19b differ from one another by one nucleotide (supplemental Figure 1B) and previous studies have suggested that these miRNAs exert a similar oncogenic function.[22] In accordance with these studies, miR-19a (supplemental Figure 1A) was retrovirally expressed in newborn mice. Quantitative PCR revealed a 20-fold increase in miR-19a expression, compared with empty vector control mice (supplemental Figure 4A). These mice also displayed splenomegaly (supplemental Figure 4B) and a significant increase in the number of $B220^+$ B-lymphocytic cells compared with control spleens (supplemental Figure 4C). However, miR-19a–overexpressing mice did not develop B-cell lymphoma, when observed during a 4-month time period, which is consistent with the previously mentioned cooperation between this miRNA and c-Myc during lymphogenesis.[22,23]

MiR-92a regulates target genes involved in erythroleukemogenesis

Because miR-17-92 induces erythroleukemia in *p53* knockout[11] and not wild type mice, we hypothesized that miR-92a modulates expression of genes responsible for erythroleukemogenesis, and

A

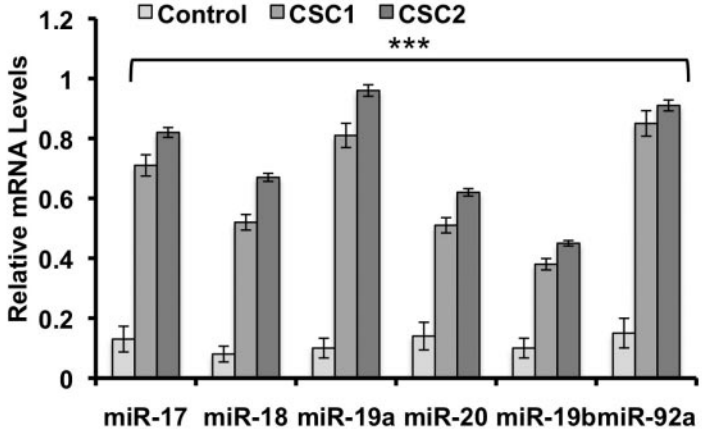

B

Marker (%)	CSC1	CSC2
c-kit+/Sca1+/ CD135+	98.1 ± 0.4	96.1 ± 0.3
c-kit+/Sca1+/ CD34+	96.2 ± 0.4	0.4 ± 0.2
CD48-/CD150-/ CD135+	94.4 ± 0.6	95.4 ± 0.3
CD41	90.0 ± 1.6	71.9 ± .1
CD38	87.0 ± 1.2	79.2 ± 1.1
CD4	4.8 ± 0.4	4.9 ± 0.5
CD8	1.2 ± 0.3	1.7 ± 0.2
Gr1+/CD11b+	0.4 ± 0.1	0.8 ± 0.2
CD71+/Ter119+	0.1 ± 0.1	0.4 ± 0.2
B220+/IgM-	2.3 ± 0.4	2.7 ± 0.1

C

Colony Type	Colony numbers
CFU-GEMM	5 ± 1.2
CFU-G	41 ± 12
CFU-M	86 ± 10
BFU-E	35 ± 6

D

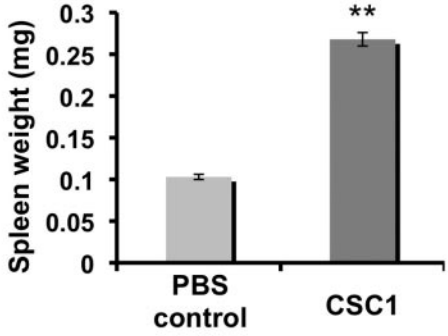

E

Marker (%)	Uninfected	PBS control	CSC1
Sca1+/ c-kit+/Lin-	0.09±0.2	0.09±0.3	11.0 ± 0.2*
Sca1+/ c-kit+/CD34+	0.02 ± 0.2	0.02 ± 0.3	4.0 ± 0.1*
Sca1+/ c-kit+/CD34-	0.01 ± 0.2	0.01 ± 0.3	0.01 ± 0.2
CD4	0	0	21.1 ± 2.0*
CD8	0	0	10.8 ± 1.2*
B220/IgM-	0	0	17.2 ± 1.4*
Gr1+/ CD11b+	13.6 ± 0.3	13.5 ± 0.2	15.7 ± 0.3
CD71+/ Ter119-	17.6 ± 0.6	17.5 ± 0.2	23.5 ± 0.7*

F

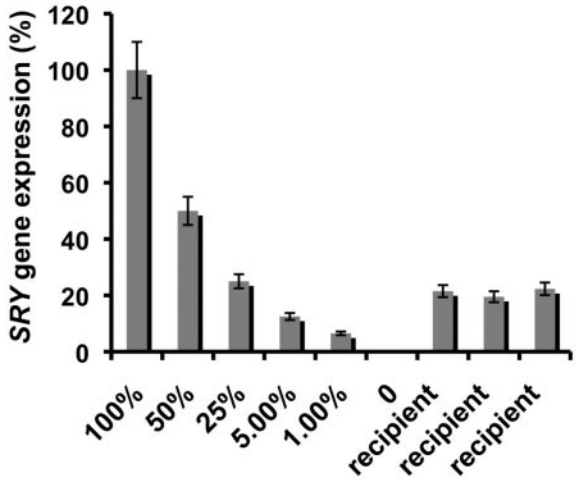

Figure 2. Characterization of multipotent hematopoietic progenitors isolated from spleens of miR-17-92–overexpressing mice. (A) Quantitative RT-PCR analysis of precursor miR-17-92 expression in CSC1 and CSC2 cell lines. Results were normalized relative to β-actin expression in all experimental samples. Each experiment was performed in quadruplicate, where error bars represent SD; ***$P < .0005$. (B) Frequency of hematopoietic cell surface marker expression, as a percentage of total CSC1 and CSC2 cell lines (n = 4), empty vector control (n = 4), and miR-17-92 mice (n = 4). Values represent the mean % ± SD. (C) Numbers of CSC1 colonies (CFU-GEMM, BFU-E, and CFU-GM) observed in an in vitro colony formation assay on methylcellulose. Colony counts were performed in triplicate after 5 days of culture. Values represent the mean ± SD detected in 3 separate experiments. (D) Average spleen weights of PBS control (n = 6) and CSC1 transplanted NOD/SCID mice (n = 8), where error bars represent SD and **$P < .005$. (E) Flow cytometric analysis using the indicated hematopoietic markers revealed reconstitution of T ($CD4^+/CD8^+$) and B ($B220^+/CD19^+$) lymphocytes in NOD/SCID mice injected with 5×10^6 CSC1 cells (n = 4), 4 months after injection. Uninfected (n = 3), and PBS-injected mice (n = 4) were used as controls. Values represent the mean % ± SD; *$P < .05$. (F) Quantitative RT-PCR analysis of CSC1 donor DNA in 3 female NOD/SCID mice transplanted with CSC1 cells. Serial dilutions of CSC1 DNA were added to normal spleen DNA and used to quantify the percentage of donor DNA, by examination of the Y chromosome specific *SRY* gene, where error bars represent SD.

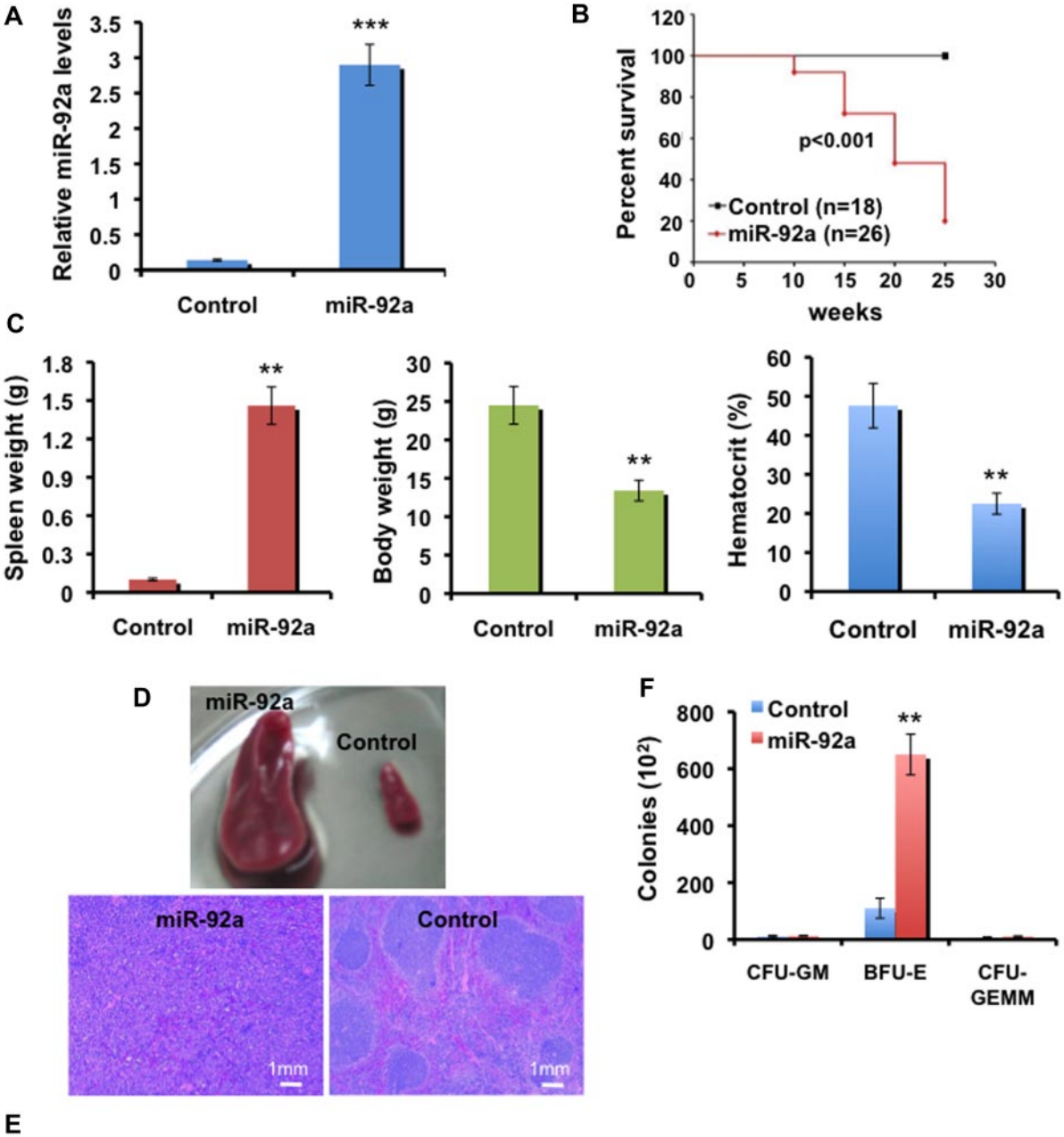

E

Mice	CD71	c-kit	CD4	CD8	B220	CD11b	Ter119	c-kit+/CD71+/ Ter119-
Uninfected	27±1.6	5±0.2	13±0.2	6±0.2	55±1.5	6±0.4	12±2.4	3.2±0.1
control	28±1.2	6±0.8	12±0.5	7±0.1	54±1.6	7±0.8	15±2.1	3.2±0.2
miR-92a	87±0.5*	71±0.4*	0.4±0.1*	5±0.6	1.6±1.2*	26±0.7*	1.3±0.3*	63.1±1.3*

Figure 3. Mice overexpressing miR-92a develop erythroleukemia. (A) Quantitative RT-PCR analysis of precursor miR-92a expression in the spleens of empty vector control (n = 6) and miR-92a mice, where n = 4, 12 weeks after infection. Results were normalized relative to β-actin expression in all experimental samples. Experiments were performed in quadruplicate, where error bars represent SD; ***$P < .0005$. (B) Survival analysis of mice injected with miR-92a (n = 26) or empty vector control (n = 18), in 3 independent experiments. (C) miR-92a overexpression (n = 8) leads to the development of leukemia associated with characteristic disease symptoms of increased spleen weight, and reduced body weights/hematocrit levels, where error bars represent SD; **$P < .005$. (D) Representative photograph of spleens from empty vector control and miR-92a mice 12 weeks after infection (top panel). H&E stained paraffin sections of isolated spleens from 12-week-old mice injected with miR-92a and empty vector control retroviruses (scale bar, 1 mm). Data are representative sections from 3 staining experiments (bottom panels). (E) Frequency of hematopoietic cell surface marker expression 6 weeks after infection, as a percentage of total splenocytes isolated from uninfected, empty vector control and miR-92a injected mice, where n = 5. Values represent the mean % ± SD; *$P < .05$. (F) Numbers of CSC1 colonies (CFU-GEMM, BFU-E, and CFU-GM) observed in an in vitro colony formation assay on methylcellulose for the indicated groups (n = 5), where error bars represent SD; **$P < .005$. Colony counts were performed in triplicate after 5 to 14 days of culture.

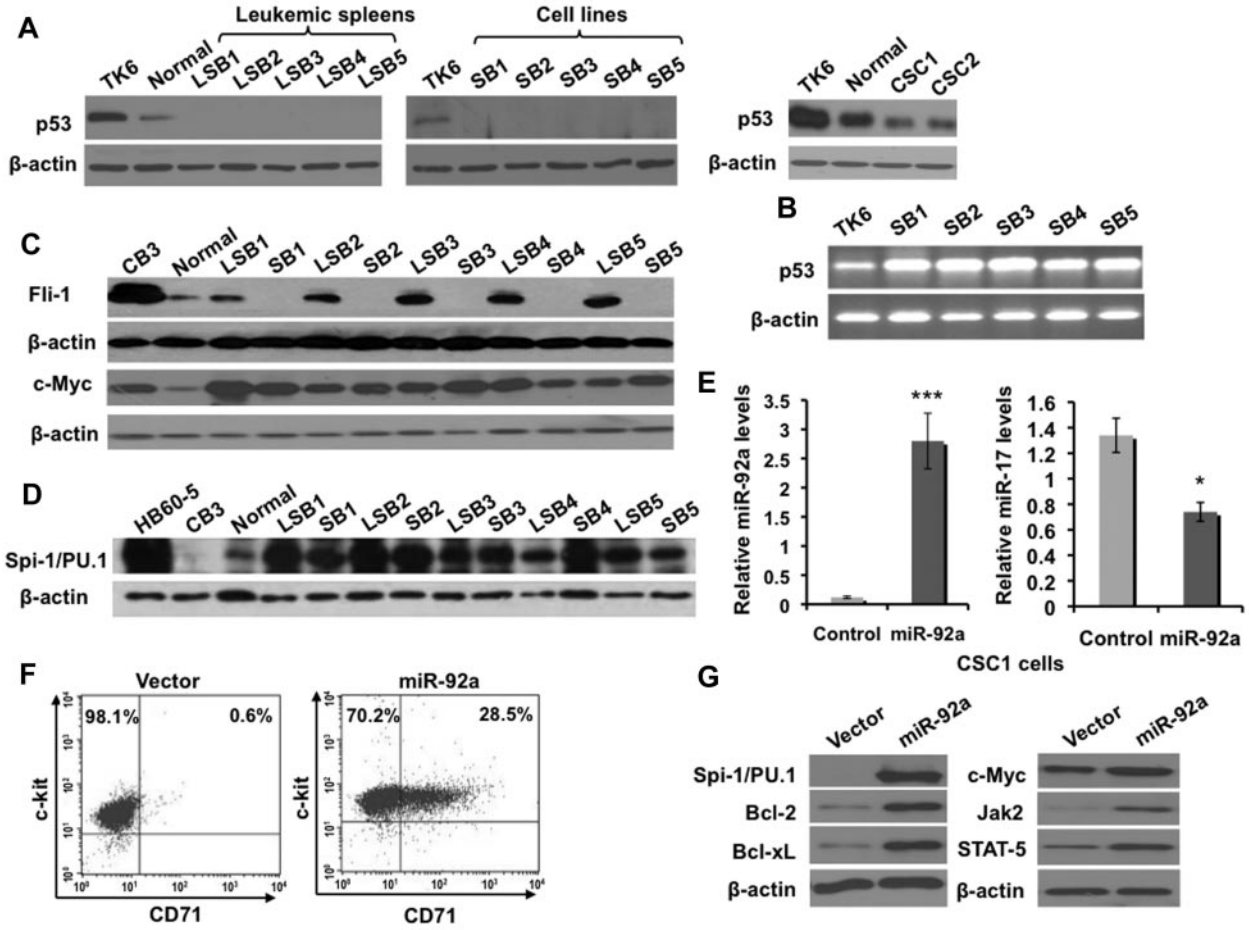

Figure 4. Overexpression of miR-92a leads to altered expression of genes involved in erythroleukemogenesis. (A) p53 protein levels in miR-92a–induced erythroleukemic spleens 1 to 5 (leukemic LSB1-5), cell lines derived from these tumors (SB1-SB5), and the miR-17-92–overexpressing cell lines CSC1 and CSC2. Levels of p53 were compared with normal spleens (Normal) and the TK6 cell line, known to express p53. (B) p53 mRNA levels were detected in SB1-SB5 and control TK6 cells by RT-PCR. (C-D) Expression of Spi-1/PU.1 (C) c-Myc, and Fli-1 (D) in erythroleukemias LSB1-LSB5 and cell lines SB1-SB5. Normal splenocytes and erythroleukemic cell lines HB60-5 and CB3 were used as controls. (E) Quantitative RT-PCR analysis of precursor miR-92a (left panel) and miR-17 (right panel) expression in pooled-populations of CSC1 cells infected with miR-92a or vector control retroviruses. Results were normalized relative to β-actin expression in all experimental samples. Each experiment was performed in quadruplicate, where error bars represent SD; $^{*}P < .05$, $^{***}P < .0005$. (F) Flow cytometric analysis revealed that miR-92a overexpressing CSC1 cells contain a significantly higher number of CD71^{+} erythroid cells relative to vector alone-infected cells. (G) CSC1 cells infected with miR-92a or vector alone retroviruses were subjected to Western blot analysis using the indicated antibodies.

functionally inactivates the p53 pathway. Indeed, erythroleukemias induced by miR-92a and corresponding cell lines SB1-SB5 lost expression of p53 protein, but not mRNA (Figure 4A-B). Accordingly miR-17-92–overexpressing cell lines CSC1 and CSC2 continue to express p53 (Figure 4A). Because the activation of the Ets transcription factors *fli-1* and *spi-1* (or *PU.1*) is a critical step in the development of erythroleukemias induced by Friend virus,[24,25] we examined whether miR-92a overexpression also affected the expression of these transcription factors. The miR-92a–induced leukemic cell lines, SB1-SB5, do not express Fli-1 (Figure 4C); however, a significant increase in the expression of Spi-1 was observed (Figure 4D). Elevated levels of c-Myc were also detected (Figure 4C), consistent with recent reports suggesting cooperation between c-Myc and miR-17-92 in the pathogenesis of lymphoma.[5]

We predicted that miR-92a overexpression, would result in differentiation of the miR-17-92–overexpressing multipotent hematopoietic progenitor cell line, CSC1, toward the erythroid pathway and development of erythroleukemia. To address this possibility, CSC1 cells were transduced with retrovirus expressing miR-92a or empty vector control, sorted based on green fluorescence, and cultured for 2 weeks in the presence of SCF and Epo. Quantitative PCR confirmed a 15-fold increase in the expression of miR-92a relative to empty vector control CSC1 cells overexpressing miR-17-92 (Figure 4E left panel). These cells also display decreased expression of tumor suppressor miR-17 (Figure 4E right panel). Flow cytometric analysis revealed that the percentage of c-kit^{+}/CD71^{+} cells increased in CSC1 cells overexpressing miR-92a, suggesting differentiation toward the erythroid lineage (Figure 4F). To determine the mechanism of erythroid expansion in miR-92a overexpressing CSC1 cells, we examined the expression of genes whose aberrant regulation has been previously implicated in erythroleukemogenesis. Correspondingly, overexpression of miR-92a in CSC1 cells resulted in the up-regulation of c-Myc and Spi-1/PU.1 as well as Bcl-2, Bcl-xl, STAT-5, and Jak2 (Figure 4G).

To gain further insight into the molecular mechanisms underlying the shift to erythropoiesis and erythroid transformation in miR-92a–overexpressing mice, we used an in silico approach to predict miR-92a target genes.[26] Among the targets identified, we focused on those known to be involved in erythroleukemogenesis, *gata-1* and *p53*.[27,28] Decreased levels of p53 and Gata-1 proteins were detected as a result of mir-92a overexpression (Figure 5A), although no visible changes in mRNA levels were noted (Figure 5B), indicating post-transcriptional regulation. The direct regulation of *p53* by miR-92a was confirmed by cloning the

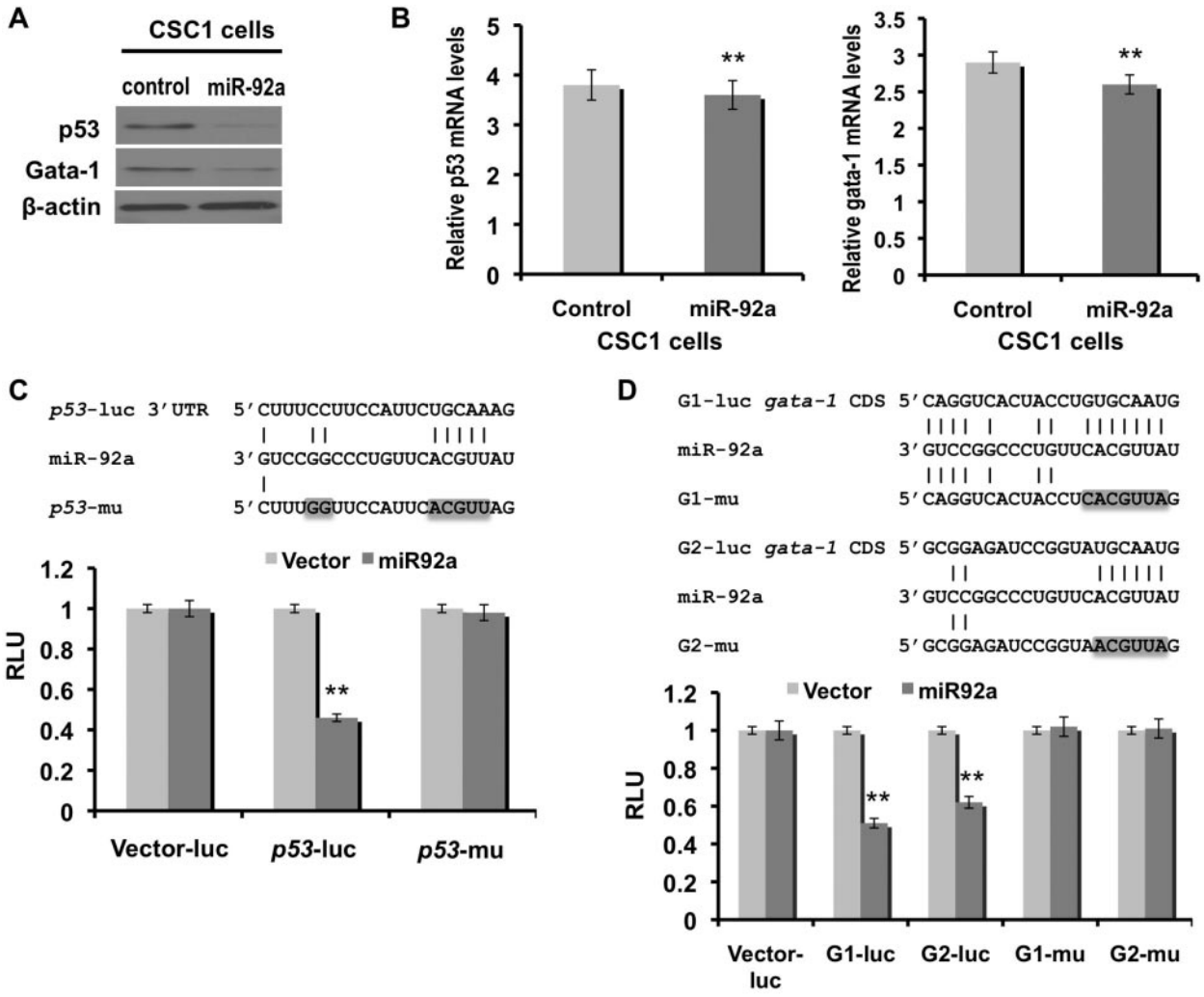

Figure 5. Gata-1 and p53 are direct targets of miR-92a. Gata-1 and p53 (A) protein and (B) quantitative mRNA expression in empty vector control and miR-92a overexpressing CSC1 cells, where error bars represent SD; $^{**}P < .005$. (C) Schematic representation (top panel) of the *p53* 3′UTR sequence containing potential miR-92a binding sites. Positions of mutations generated (*p53*-mu) are marked in gray. Luciferase assay (bottom panel) of the reporter vector containing the *p53* binding site and its corresponding mutation (*p53*-mu) after transient transfection in NIH-3T3 cells stably expressing miR-92a. (D) Schematic representation (top panel) of the *gata-1* CDS containing potential miR-92a binding sites (G_1 and G_2). Positions of mutations generated within G_1 (G1-mu) and G_2 (G2-mu) are marked in gray. Luciferase assay (bottom panel) of the reporter genes containing the G_1 or G_2 binding sites and their corresponding mutations (G1-mu or G2-mu) after transient transfection in NIH-3T3 cells stably expressing miR-92a. The expression is presented relative to that obtained with transfection of control vector alone. Error bars represent SD; $^{**}P < .005$.

potential conserved miR-92a binding site, located within the 3′UTR of *p53*, into a luciferase reporter construct (*p53*-luc; Figure 5C, top panel). A construct in which the p53 target sequence was mutated (*p53*-mu), was used as a control (Figure 5C top panel). The luciferase constructs *p53*-luc or *p53*-mu were transiently transfected into NIH-3T3 cells stably expressing miR-92a or the empty vector. As shown in Figure 5C (bottom panel), miR-92a significantly decreased the luciferase activity of *p53*-luc transfected cells, but did not affect luciferase activity of the *p53*-mutant transfected cells.

Although a miR-92a seed sequence match was not identified in the 3′UTR of *gata-1*, down-regulated protein expression and unchanged mRNA levels in miR-92a–overexpressing mice (Figure 5A-B right panel), is suggestive of *gata-1* post-transcriptional regulation. Since naturally occurring miRNA targets in amino acid coding sequences (CDS) have been reported,[29] we assessed the CDS of *gata-1* and identified 2 potential conserved miR-92a binding sites (Figure 5D top panel). Luciferase assays using NIH-3T3 cells overexpressing miR-92a revealed decreased activity of the reporter construct containing the 2 putative miR-92a binding sites (G_1, G_2) within the *gata-1* CDS (Figure 5D top panel). However, miR-92a did not affect the luciferase activity of G1 or G2-mutant transfected cells, which suggests direct targeting of *gata-1* by miR-92a (Figure 5D bottom panel).

MiR-17 suppresses the oncogenic function of miR-92a

The previously mentioned results demonstrated, for the first time, that miR-92a is a potent inducer of erythroleukemia in mice, whereas overexpression of miR-17-92 leads to the expansion of multipotent hematopoietic progenitors. This observation led us to hypothesize that individual miRNA units within this cluster may block miR-92a–induced erythroleukemia development. Although the oncogenic function of miR-18 has not yet been established, recent reports have demonstrated that deregulated miR-17 and miR-20 expression inhibits cellular invasion, tumor metastasis, and proliferation.[30,31] We therefore assessed the ability of miR-17 to inhibit miR-92a–induced erythroleukemogenesis by injecting newborn mice with retroviruses expressing miR-17, miR-92a, or miR-17 and miR-92a together. These studies indicated that miR-17

overexpression alone does not impact mouse survival, body weight, spleen size, or hematocrit levels (supplemental Figure 5A). Although miR-92a overexpression led to erythroleukemia development, coexpression of miR-92a and miR-17 (supplemental Figure 5B,C) led to suppression and longer latency period, but not the prevention of erythroleukemia (Figure 6A). Flow cytometric analysis revealed that these mice displayed a significant reduction in the number of c-kit$^+$ and CD71$^+$ erythroleukemic cells (supplemental Table 2).

To determine the underlying mechanism of leukemic inhibition by miR-17, this microRNA was overexpressed in the SB1 miR-92a–induced erythroleukemia cell line (Figure 6B). SB1 cells, overexpressing miR-17, displayed a significantly reduced proliferation rate, compared with the parental cell line (Figure 6C). Cell cycle analysis using PI revealed an increase in the proportion of sub-G_1 cells, suggesting apoptotic death (supplemental Figure 6A). These cells exhibited morphological features of apoptosis, and ultimately died 2 weeks after transduction (supplemental Figure 6B). Interestingly, miR-17 overexpression also led to the up-regulation of the oncogenic miR-92a target p53, whereas Gata-1 expression remained unchanged (Figure 6D).

MiR-17 down-regulates expression of genes involved in erythroid proliferation

To further characterize the ability of miR-17 to abrogate the onset of miR-92a–induced erythroleukemia, we used an in silico approach to predict miR-17 target genes. Among the putative targets identified, the erythroid-related survival genes *bcl-2*, *STAT-5*, and *jak2* have at least one complementary site to the miR-17 seed region within their 3′UTR. Western blot analysis revealed reduced levels of Bcl-2, STAT-5 and Jak2 protein in miR-17 overexpressing SB1 cells (Figure 6E), whereas mRNA transcript levels remained unaffected (supplemental Figure 7), suggesting post-transcriptional regulation. To assess the ability of miR-17 to directly regulate the expression of these genes, NIH-3T3 cells stably expressing miR-17 were cotransfected with a *bcl-2* 3′UTR luciferase vector (*bcl-2*-luc), luciferase reporter vector control (vector-luc), or the construct in which the miR-17 target site was mutated (*bcl-2*-mu; Figure 6F top panel). MiR-17 expression significantly decreased luciferase activity in *bcl-2*-luc transfected cells, but not in *bcl-2*-mutant transfected cells (Figure 6F bottom panel). Analogous experiments revealed that miR-17 also inhibited STAT-5 and Jak2 expression through conserved binding sites located within their 3′UTR (Figure 6G-H). Taken together these data indicate that miR-17 directly regulates survival proteins Bcl-2, STAT-5, and Jak2, which may, at least in part, account for the tumor-suppressive function of miR-17.

Imbalanced expression of individual miR-17-92 units is associated with the loss of p53

Because the overexpression of miR-17-92 induces erythroleukemia in p53 knockout mice,[11] we hypothesized that p53 inactivation triggers the imbalanced expression of individual miR-17-92 members. To investigate this possibility, the expression of each miR-17-92 member was examined in Friend virus-induced erythroleukemic cell lines KH9 and KH16 induced in *p53*$^{-/-}$ mice, carrying a retroviral activated, and amplified miR-17-92 region, respectively.[11] Quantitative-PCR analysis revealed that these cell lines express elevated levels of miR-92a, and decreased levels of miR-17, compared with other miR-17-92 members, and relative to normal spleens (Figure 7A). Imbalanced expression of miR-17-92 members was also detected in several p53 negative murine and human erythroleukemia cell lines (data not shown). Similarly, miR-92a–overexpressing CSC1 cells, displaying erythroid expansion (Figure 4F) associated with p53 down-regulation (Figure 5A), express lower levels of tumor suppressive miR-17 compared with CSC1 vector control cells (supplemental Figure 7B). Correspondingly, the use of antisense technology to down-regulate p53 expression in CSC1 cells resulted in a marked shift toward the erythroid lineage and increased miR-92a and decreased miR-17 expression (supplemental Figure 8 A-C), suggesting that p53 is a critical miR-92a target driving erythroid transformation.

We used a temperature sensitive mutant *p53* allele in which the alanine at position 135 was changed to valine.[32] At 37°C this *p53*$^{Val-135}$ allele undergoes a conformational change to act as a mutant protein becoming mainly cytoplasmic and bound to hsc70 protein causing growth arrest, but not at 32°C when it mimics wild-type p53.[32] When cultured at 32°C, SB1 cells transduced to express the *p53*$^{Val-135}$ allele display enhanced p21 expression, and marked growth inhibition (Figure 7B-C), thereby rescuing the leukemic phenotype. Accordingly, quantitative RT-PCR revealed an increase in tumor suppressive, and decrease in the oncogenic miR-17-92 members (Figure 7D), confirming the p53 relationship.

To further corroborate these findings in a clinical setting, we examined the expression of miR-17-92 in B-cell CLL (B-CLL), the most common type of leukemia. Although B-CLL patients display several genetic aberrations that impact disease, those carrying deletions in the short arm of chromosome 17p on which *p53* is located, present with significantly more aggressive disease and shorter survival.[33] In accordance with our previous results, B-CLL patients lacking p53 expression and displaying aggressive disease, exhibited reduced miR-17 and miR-20 expression, and increased miR-19a/b and miR-92a expression, whereas miR-18 levels remain unchanged, relative to healthy normal controls (Figure 7E, supplemental Table 3). This expression pattern was designated the p53$^-$ signature. In contrast, patients representative of the 17p$^+$ group, expressing wildtype p53, exhibited increased levels of miR-17 and miR-20, unchanged levels of miR-18, miR-19a/b and lower levels of miR-92a, designated the p53$^+$ signature (Figure 7F, supplemental Table 4). Interestingly, 6 patients (Nos. 7, 8, 10-13) exhibiting the p53$^-$ signature, do not carry the 17p deletion, and 2 patients (Nos. 3, 28) exhibiting the p53$^+$ signature, carry the 17p deletion (supplemental Table 3). To explain this phenomenon, B-CLL cells were irradiated for examination of p53 functional status. On exposure to ionizing radiation, p53 expression up-regulated its target gene *p21*. B-CLL patients 7, 8, and 10-13 were characterized as functionally inactive for p53 as irradiation of B-CLL cells failed to induce the expression of this tumor-suppressor gene as well as its target gene *p21* (select data, supplemental Figure 9A). In B-CLL patients 3 and 28, p53 was functionally active because irradiation induced expression of both p53 and p21 (supplemental Figure 9B). These results further confirm that the loss of p53 expression or function contributes to deregulated expression of individual miR-17-92 members in hematopoietic malignancies leading to overexpression of oncogenic miRNAs.

Discussion

This study contributes to our working knowledge of miRNA oncogenic and tumor suppressive function, and the direct consequences of aberrant miRNA expression on tumorigenesis. Herein, we discovered that miR-17-92 overexpression in mice results in

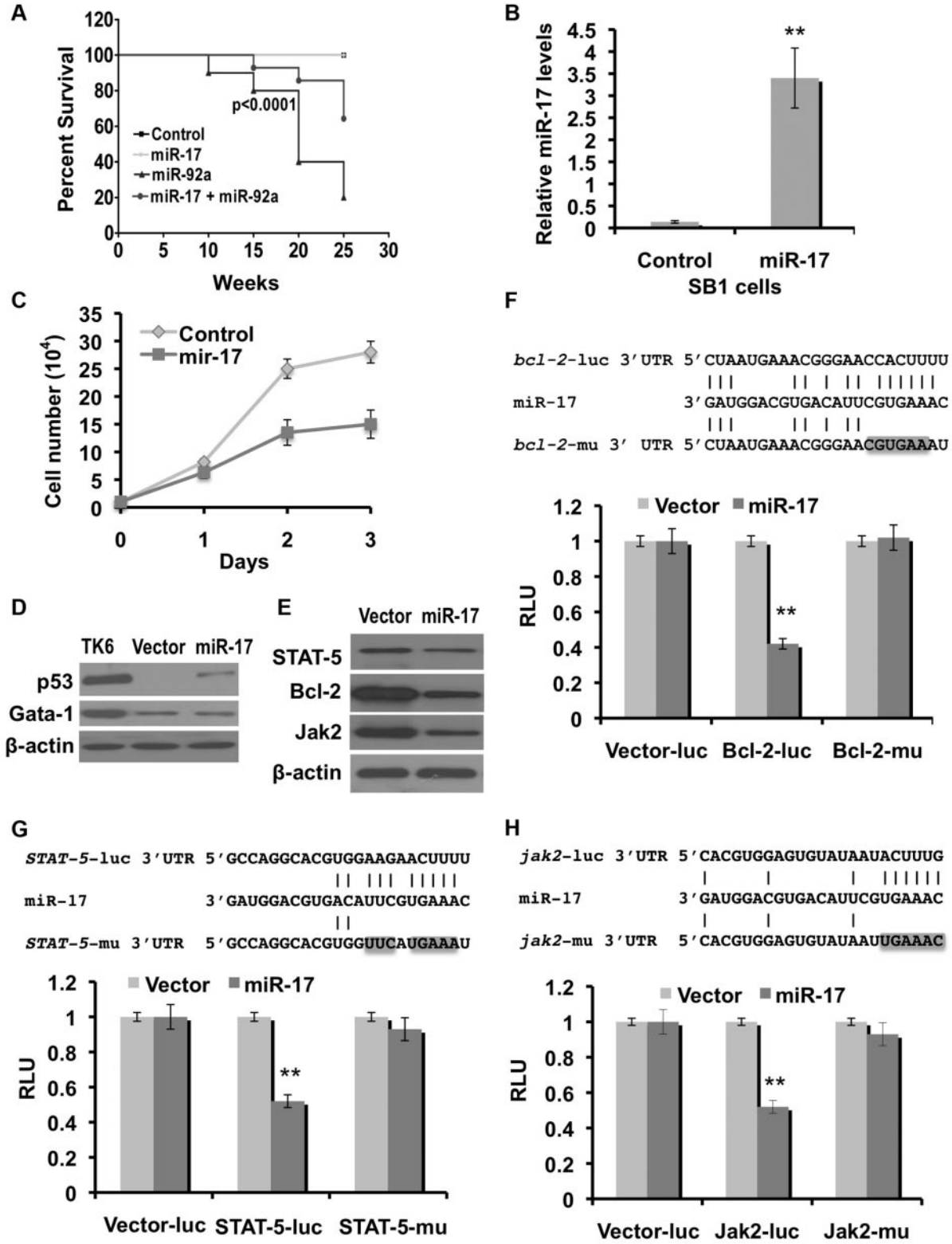

Figure 6. Suppression of miR-92a–induced erythroleukemogenesis by miR-17 is associated with target gene down-regulation. (A) Survival analysis of mice injected with miR-92a (n = 20), miR-17 (n = 18), miR-17+miR-92a (n = 26) and empty vector control (n = 17) retroviruses. (B) Quantitative RT-PCR analysis of precursor miR-17 expression in pooled-populations of SB1 cells infected with miR-17 or empty vector retroviruses. Results were normalized relative to β-actin expression in all experimental samples. Each experiment was performed in quadruplicate, where error bars represent SD; $^{**}P < .005$. (C) Proliferation rates of miR-17 and control vector infected SB1 cells, as determined on the indicated days using the Trypan blue exclusion assay. (D) p53, Gata-1, (E) STAT-5, Bcl-2, and Jak2 protein expression in SB1 cells transduced with miR-17 or control vector retroviruses. TK6 cells were used as a positive control for p53 expression. Schematic representation (top panel) of the *bcl-2* 3′UTR (E), *STAT-5* 3′UTR (F), and *jak2* 3′UTR (G) containing potential miR-17 binding sites. Positions of mutations generated within these binding sites (*bcl-2*-mu, *STAT-5*-mu, and *jak2*-mu) are indicated in gray. Luciferase assays (bottom panel) of the reporter vector containing the *bcl-2* 3′UTR (E), *STAT-5* 3′UTR (F), *jak2* 3′UTR (G), and their corresponding mutations after transient transfection in NIH-3T3 cells stably expressing miR-17. Data are representative of 5 separate experiments, where error bars represent SD; $^{**}P < .005$. The expression is presented relative to that obtained with transfection of control vector alone.

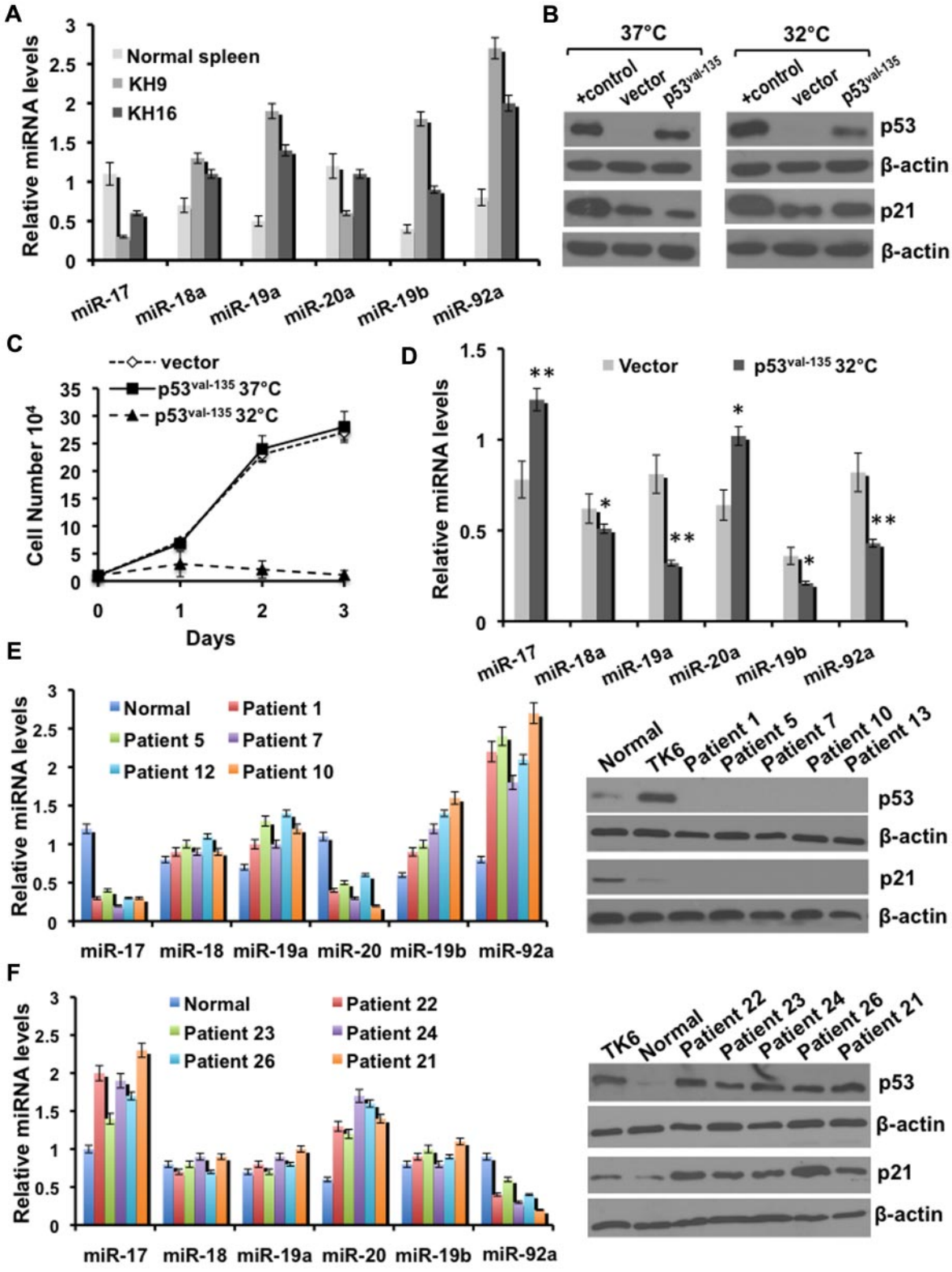

Figure 7. Imbalanced expression of the individual members of miR-17-92 is associated with the loss of p53. (A) Quantitative RT-PCR analysis of individual precursor miR-17-92 expression in the KH9 and KH16 erythroleukemic cell lines derived from *p53*$^{-/-}$ mice, relative to normal spleens. Each experiment was performed in quadruplicate, where error bars represent SD. (B) p53 and p21 protein expression in SB1 cells transduced to express the p53$^{Val-135}$ allele or empty vector cultured at 37°C and 32°C, where β-actin was used as a loading control. TK6 human B-lymphoblastoid and NIH-3T3 cells were used as positive controls (+control) for p53 and p21 expression, respectively. (C) Proliferation rates of empty vector control and p53$^{Val-135}$ transduced SB1 cells, as determined on the indicated days using the Trypan blue exclusion assay. Quantitative RT-PCR analysis of individual precursor miR-17-92 expression in (D) empty vector control and p53$^{Val-135}$ transduced SB1 cells cultured at 32°C, and (E-F left panel) indicated B-CLL patients displaying a p53^{-} and p53^{+} signature, respectively. Each experiment was performed in quadruplicate, where error bars represent SD; $^{*}P < .05$, $^{**}P < .005$. (E-F right panel) p53 and p21 protein expression in the indicated B-CLL patient samples, where β-actin was used as a loading control. B cells isolated from 5 normal healthy volunteers and the p53^{+} TK6 cells were used as controls.

splenomegaly and expansion of a multipotent hematopoietic progenitor population. In contrast, overexpression of miR-19a or miR-92a alone results in B-cell lympho-proliferation and erythroleukemia, respectively. Interestingly, miR-92a–induced erythroleukemia development is abrogated by coexpression of miR-17. These results establish both tumor-promoting and tumor-suppressing roles for individual members of the miR-17-92 cluster.

CSC1 and CSC2 cell lines derived from miR-17-92–overexpressing mice resemble a heterogeneous population of cells containing multipotent progenitors, suggesting that this miRNA cluster may also increase the self-renewal capacity of hematopoietic stem cells or committed progenitors. Consistent with this study, it has been previously shown that miR-17-92 is expressed in hematopoietic stem cells and cancer initiating cells.[4,6,34] Interestingly, this cluster is also among a handful of genes necessary and sufficient to convert differentiated cells to induced pluripotent stem (iPS) cells.[35]Thus, further investigation into the mechanism of miR-17-92–induced expansion of multipotent hematopoietic progenitors may provide new insight into the pathways governing self-renewal and transformation of hematopoietic progenitors.

We further clarified the tumor-promoting ability of miR-92a by identifying 2 targets *p53* and *gata-1*. Down-regulation of *gata-1* in miR-92a–induced erythroleukemias is consistent with the critical role this gene plays in erythroid proliferation and differentiation,[29] and loss of p53 is frequently detected in numerous aggressive cancers and accelerates erythroleukemogenesis induced by Friend virus.[36] In addition, miR-92a–induced erythroleukemia cells display elevated expression of oncogenes, *spi-1/PU.1* and *c-myc*, whose aberrant expression is frequently detected in various cancers including several hematologic malignancies.[2,25] Ectopic overexpression of miR-92a in the multipotent progenitor cell line CSC1 induced differentiation toward the erythroid lineage, down-regulated p53 and Gata-1, and up-regulated Spi-1/PU.1 and c-Myc. Moreover, these cells display elevated expression of Bcl-2, STAT-5, and Jak2, factors involved in erythroid transformation,[37,38,39] likely contributing to miR-92a–induced erythroleukemia. Thus, it is conceivable that miR-92a-mediated inhibition of p53 and Gata-1 acts in synergy with up-regulation of Spi-1/PU.1 and c-Myc to transform erythroid progenitors in mice only 5 weeks after injection.

Interestingly, miR-17 acts as a tumor-suppressor, blocking pathways that promote erythroid transformation. We have shown that miR-17 slows the progression of miR-92a–induced erythroleukemogenesis, at least in part, by direct inhibition of Bcl-2, STAT-5, and Jak2. Down-regulation of these survival factors resulted in inhibition of proliferation and induction of apoptosis. In support of this observation, a recent report also noted down-regulation of STAT-3 by miR-17 as the key gene that inhibits cellular invasion and tumor metastasis.[40] Interestingly, we have also shown that these survival genes are up-regulated in miR-92a-erythroleukemia, further demonstrating the importance of these genes in erythroid transformation. The ability of individual miR-17-92 components to inhibit expression of specific target genes leading to their ability to function as an oncogene or tumor-suppressor gene is summarized in supplemental Figure 10.

Both miR-92a and miR-17 regulate distinct tumor-suppressor and growth promoting genes, respectively, through direct binding within their 3′UTR or CDS. The dichotomous roles of these miRNAs suggest that imbalanced expression of individual miR-17-92 members leads to malignant transformation through the oncogenic units of this cluster. Our study demonstrated that although miR-17-92 activation promotes erythroleukemia in *p53* knockout mice,[11] wild-type mice infected with this cluster remain free of disease. Erythroleukemia cell lines derived from these $p53^{-/-}$ mice overexpressing miR-17-92 displayed high miR-92a and low miR-17 levels. Moreover, miR-92a overexpressing multipotent CSC1 cells, in which p53 expression was directly down-regulated, demonstrated imbalanced expression of individual miR-17-92 members.

The above observations were further supported by down-regulating p53 in CSC1 cells and expressing this tumor suppressor gene in miR-17-92 overexpressing erythroleukemic cells. These results suggest that the loss of p53 in erythroid progenitors is at least in part responsible for the imbalanced expression of miR-17-92, leading to erythroleukemogenesis.

The relationship between p53 and imbalanced miR-17-92 expression was also observed in various human-derived leukemic cells and B-CLL patient samples, where increased expression of oncogenic miR-17-92 members and decreased expression of tumor suppressive members probably contributes to accelerated disease progression. Because inactivation of p53 is a common genetic event in many cancers,[41] imbalanced expression of individual miR-17-92 units may play a critical role in the progression of broad range tumors carrying a p53 dysfunction. Accordingly, p53 has recently been demonstrated to interact with the Drosha miRNA processing complex through association with DEAD-box RNA helicase p68, facilitating the processing of primary miRNAs to precursor miRNAs.[42] The loss of p53 may selectively effect the processing of miR-17-92 miRNA, resulting in the imbalanced expression of its encoded units. It is therefore conceivable that in tumors overexpressing or carrying an amplified miR-17-92 locus, collaboration with preexisting mutations is necessary to generate imbalanced expression of different units of this cluster to convert the premalignant to a malignant phenotype. Further examination into the expression pattern of different units of the miR-17-92 cluster can potentially be exploited for diagnosis and treatment of cancers displaying *miR-17-92* gene amplification. Further characterization of miR-17-92 and its individual units may increase our understanding of basic mechanisms of hematopoietic cell regulation and assist us in developing novel and efficient molecular targets for modulating the hematopoietic compartment, and conversely, inhibit malignant growth.

Acknowledgments

The authors thank Melanie Suttar for her excellent secretarial assistance.

This work was supported by a grant from the Leukemia & Lymphoma Society of Canada and the Canadian Institute of Health Research to Y.B.-D. (MOP-110952).

Authorship

Contribution: Y.L. performed the experiments, and with the assistance of L.M.V.-F. wrote the paper and analyzed the data; Y.-J.L. performed the luciferase experiments; S.E.E. assisted in data analysis and the critical review of the paper; D.S. provided CLL patient samples and was involved in CLL patient analysis; M.R.H. analyzed the hematopoietic progenitor and flow data; and Y.B.-D. was responsible for the supervision and data analysis.

Conflict-of-interest disclosure: The authors declare no competing financial interests.

Correspondence: Yaacov Ben-David, Sunnybrook Health Sciences Centre, Division of Molecular and Cellular Biology, Room S-216, 2075 Bayview Avenue, Toronto, ON, M4N 3M5 Canada; e-mail: bendavid@sri.utoronto.ca.

References

1. Chen CZ, Li L, Lodish HF, Bartel DP. 2004. MicroRNAs modulate hematopoietic lineage differentiation. *Science.* 2004;303(5654):83-86.
2. Delgado MD, León J. Myc roles in hematopoiesis and leukemia. *Genes Cancer.* 2010;1(6):605-616.
3. Koralov SB, Muljo SA, Galler GR, et al. Dicer ablation affects antibody diversity and cell survival in the B lymphocyte lineage. *Cell.* 2008;132(5):860-874.
4. Xiao C, Srinivasan L, Calado DP, et al. Lymphoproliferative disease and autoimmunity in mice with increased miR-17-92 expression in lymphocytes. *Nat Immunol.* 2008;9(4):405-414.
5. He L, Thomson JM, Hemann MT, et al. A microRNA polycistron as a potential human oncogene. *Nature.* 2005;435(7043):828-833.
6. Mi S, Li Z, Chen P, et al. Aberrant overexpression and function of the miR-17-92 cluster in MLL-rearranged acute leukemia. *Proc Natl Acad Sci U S A.* 2010;107(8):3710-3715.
7. Calin GA, Sevignani C, Dumitru CD, et al. Human microRNA genes are frequently located at fragile sites and genomic regions involved in cancers. *Proc Natl Acad Sci U S A.* 2004;101(9):2999-3004.
8. Lu J, Getz G, Miska EA, et al. MicroRNA expression profiles classify human cancers. *Nature.* 2005;435(7043):834-838.
9. Bartel DP. MicroRNAs: genomics, biogenesis, mechanism, and function. *Cell.* 2004;116(2):281-297.
10. Kloosterman WP, Plasterk RH. The diverse functions of microRNAs in animal development and disease. *Dev Cell.* 2006;11(4):441-450.
11. Cui JW, Li YJ, Sarkar A, et al. Retroviral insertional activation of the Fli-3 locus in erythroleukemias encoding a cluster of microRNAs that convert Epo-induced differentiation to proliferation. *Blood.* 2007;110(7):2631-2640.
12. Ota A, Tagawa H, Karnan S, et al. Identification and characterization of a novel gene, C13orf25, as a target for 13q31-q32 amplification in malignant lymphoma. *Cancer Res.* 2004;64(9):3087-3095.
13. Tagawa H, Seto M. A microRNA cluster as a target of genomic amplification in malignant lymphoma. *Leukemia.* 2005;19(11):2013-2016.
14. Hayashita Y, Osada H, Tatematsu Y, et al. A polycistronic microRNA cluster, miR-17-92, is overexpressed in human lung cancers and enhances cell proliferation. *Cancer Res.* 2005;65(21):9628-9632.
15. Hossain A, Kuo MT, Saunders GF. Mir-17-5p regulates breast cancer cell proliferation by inhibiting translation of AIB1 mRNA. *Mol Cell Biol.* 2006;26(21):8191-8201.
16. Lee Y, et al. The nuclear RNase III Drosha initiates microRNA processing. *Nature.* 2003; 425(6956):415-419.
17. Akashi K, Traver D, Miyamoto T, Weissman IL. A clonogenic common myeloid progenitor that gives rise to all myeloid lineages. *Nature.* 2000; 404(6774):193-197.
18. Mikkola HK, Fujiwara Y, Schlaeger TM, Traver D, Orkin SH. Expression of CD41 marks the initiation of definitive hematopoiesis in the mouse embryo. *Blood.* 2003;101(2):508-516.
19. Randall TD, Lund FE, Howard MC, Weissman IL. Expression of murine CD38 defines a population of long-term reconstituting hematopoietic stem cells. *Blood.* 1996;87(10):4057-4067.
20. Spaner D, Sheng-Tanner X, Raju K, Rabinovich B, Messner H, Miller RG. Long term persistence of IL-2-unresponsive allogeneic T cells in sublethally irradiated SCID mice. *Int Immunol.* 1999;11(10):1601-1614.
21. Wang X, Zhang J, Zhang YP. Erratic evolution of SRY in higher primates. *Mol Biol Evol.* 2002; 19(4):582-584.
22. Olive V, Bennett MJ, Walker JC, et al. miR-19 is a key oncogenic component of mir-17-92. *Genes Dev.* 2009;23(24):2839-2849.
23. Mu P, Han Y-C, Betel D, et al. Genetic dissection of the mir-17-92 cluster of microRNAs in Myc-induced B-cell lymphomas. *Genes Dev.* 2009; 23(24):2806-2811.
24. Ben-David Y, Giddens EG, Letwin K, Bernstein A. Erythroleukemia induction by Friend murine leukemia virus: insertional activation of a new member of the ets gene family, Fli-1, closely linked to c-ets-1. *Genes Dev.* 1991;5(6):908-918.
25. Moreau-Gachelin F, Wendling F, Molina T, et al. Spi-1/PU. 1 transgenic mice develop multistep erythroleukemias. *Mol Cell Biol.* 1996;16(5):2453-2463.
26. Krek A, Grün D, Poy MN, et al. Combinatorial microRNA target predictions. *Nat Genet.* 2005; 37(5):495-500.
27. Howard JC, Yousefi S, Cheong G, Bernstein A, Ben-David Y. Temporal order and functional analysis of mutations within the Fli-1 and p53 genes during the erythroleukemias induced by F-MuLV. *Oncogene.* 1993;8(10):2721-2729.
28. Pan X, Ohneda O, Ohneda K, et al. Graded levels of GATA-1 expression modulate survival, proliferation, and differentiation of erythroid progenitors. *J Biol Chem.* 2005;280(23):22385-22394.
29. Tay Y, Zhang J, Thomson AM, Lim B, Rigoutsos I. MicroRNAs to Nanog, Oct4 and Sox2 coding regions modulate embryonic stem cell differentiation. *Nature.* 2008;455(7216):1124-1128.
30. Yu Z, Willmarth NE, Zhou J, et al. MicroRNA 17/20 inhibits cellular invasion and tumor metastasis in breast cancer by heterotypic signaling. *Proc Natl Acad Sci U S A.* 2010;107(18):8231-8236.
31. Shan SW, Lee DY, Deng Z, et al. MicroRNA miR-17 retards tissue growth and represses fibronectin expression. *Nat Cell Biol.* 2009;11(8): 1031-1038.
32. Michalovitz D, Halevy O, Oren M. Conditional inhibition of transformation and of cell proliferation by a temperature-sensitive mutant of p53. *Cell.* 1990;62:671-680.
33. Dohner H, Stilgenbauer S, Benner A, et al. Genomic aberrations and survival in chronic lymphocytic leukemia. *N Engl J Med.* 2000;343(26): 1910-1916.
34. Georgantas RW 3rd, Hildreth R, Morisot S, et al. CD34+ hematopoietic stem-progenitor cell microRNA expression and function: a circuit diagram of differentiation control. *Proc Natl Acad Sci U S A.* 2007;104(8):2750-2755.
35. Gunaratne PH. Embryonic stem cell microRNAs: defining factors in induced pluripotent (iPS) and cancer (CSC) stem cells? *Curr Stem Cell Res Ther.* 2009;4(3):168-177.
36. Wong KS, Li YJ, Howard J, Ben-David Y. Loss of p53 in F-MuLV induced-erythroleukemias accelerates the acquisition of mutational events that confers immortality and growth factor independence. *Oncogene.* 1999;18(40):5525-5534.
37. Cui J, Vecchiarelli-Federico LM, Li Y, Wang GJ, Ben-David Y. Continuous Fli-1 expression plays an essential role in the proliferation and survival of F-MuLV-induced erythroleukemia and human erythroleukemia. *Leukemia.* 2009;23(7):1311-1319.
38. Schuringa JJ, Chung KY, Morrone G, Moore MA. Constitutive activation of STAT5A promotes human hematopoietic stem cell self-renewal and erythroid differentiation. *J Exp Med.* 2004;200(5): 623-635.
39. Khwaja A. The role of Janus kinases in haemopoiesis and haematological malignancy. *Br J Haematol.* 2006;134(4):366-384.
40. Zhang M, Liu Q, Mi S, et al. Both miR-17-5p and miR-20a alleviate suppressive potential of myeloid-derived suppressor cells by modulating STAT3 expression. *J Immunol.* 2011;186(8):4716-4724.
41. Puzio-Kuter AM, Castillo-Martin M, Kinkade CW, et al. Inactivation of p53 and Pten promotes invasive bladder cancer. *Genes Dev.* 2009;23(6):675-680.
42. Suzuki HI, Yamagata K, Sugimoto K, et al. Modulation of microRNA processing by p53. *Nature.* 2009;460(7254):529-533.